ORIGINAL PAPER

Submitted: 20.03.2024
Accepted: 21.05.2024
Early publication date: 09.08.2024

Endokrynologia Polska
DOI: 10.5603/ep.99891
ISSN 0423–104X, e-ISSN 2299–8306

The impact of glucagon and exenatide on oxidative stress levels and antioxidative enzyme expression in *in vitro* induced steatosis in HepG2 cell culture

Aleksandra Bołdys, Łukasz Bułdak, Estera Skudrzyk, Grzegorz Machnik, Bogusław Okopień

Department of Internal Medicine and Clinical Pharmacology, Faculty of Medical Sciences in Katowice, Medical University of Silesia, Katowice, Poland

Abstract

Introduction: Metabolic dysfunction-associated steatotic liver disease (MASLD) is a healthcare issue of growing concern. Its development is multifactorial, and it is more commonly seen in obese patients. In those circumstances, intracellular lipid overload ensues, resulting in oxidative stress that might be responsible for progression toward steatohepatitis. Novel therapeutic approaches that are effective in weight management are expected to improve the course of MASLD. One of the potential mechanisms involved in such protective properties may relate to the reduction in oxidative stress.

Material and methods: The induction of steatosis and the assessment of oxidative stress level and expression of antioxidant enzymes (superoxide dismutase — SOD, glutathione peroxidase — GPx and catalase — Cat) in HepG2 hepatoma cell line subjected to glucagon and exenatide treatment.

Results: Exenatide monotherapy successfully reduced lipid accumulation by 25%. Significant reductions in markers of oxidative stress (reactive oxygen species and malondialdehyde) were obtained in cells subjected to combined treatment with glucagon and exenatide (by 24 and 21%, respectively). Reduced burden of oxidative stress was associated with elevated expression of SOD and GPx but not Cat.

Conclusions: Combined activation of glucagon-like peptide-1 (GLP-1) and glucagon receptors reduces oxidative stress in HepG2 steatotic cell cultures. This observation may stem from increased antioxidative potential.

Key words: *exenatide; glucagon; GLP-1; MASLD; liver steatosis; oxidative stress; antioxidant; HepG2*

Introduction

Metabolic dysfunction-associated steatotic liver disease (MASLD) is emerging as a significant healthcare concern, estimated to affect 30% of the world population [1]. The course of the disease may lead to a myriad of systemic complications [2]. Liver cirrhosis resulting from advanced stages of MASLD accounts for up to 5% of liver transplantations in Europe and even as much as 15% in the United States [3, 4]. The initial step in the progression of MASLD is the increased fat accumulation within the liver. The main culprit in the pathogenesis appears to be an excess of free fatty acids (FFAs), which activate intracellular proinflammatory mitogen-activated protein kinases (MAPKs). This activation exacerbates oxidative stress through the generation of superoxide radicals and reactive aldehyde products [e.g. malondialdehyde (MDA)] [5]. As a result, in some patients with liver steatosis, inflammation ensues. Unfortunately, there are no well-established markers that predict the course of the disease. The imbalance in redox status has already been shown to be essential in the development of several medical conditions (including diabetes, atherosclerosis, and cancer) [6]. Oxidative stress is one of the major contributors in the progression of MASLD toward metabolic dysfunction-associated steatohepatitis (MASH) [7]. This leads to elevated expression of proinflammatory cytokines and activation of stellate cells, ultimately culminating in liver fibrosis. Cellular mechanisms that alleviate excess of reactive oxygen species (ROS) involve several enzymes with potent antioxidative properties. These include catalase (Cat) and glutathione peroxidase (GPx), which deal with hydrogen peroxide, and superoxide dismutase (SOD), which degrades reactive superoxides [8]. Restoring the oxidoreductive balance can be achieved by the improvement of antioxidant enzyme expression and/or their activity.

Previously it was found that glucagon-like peptide-1 (GLP-1) analogues can improve antioxidant capacity in human monocytes/macrophages, astrocytes, and insulin-secreting pancreatic islet beta cells [9–11].

Łukasz Bułdak, Department of Internal Medicine and Clinical Pharmacology, Faculty of Medical Sciences in Katowice, Medical University of Silesia, Medyków 18, 40–752 Katowice, Poland, tel. +48 32 242 39 02; e-mail: lbuldak@sum.edu.pl

Nowadays, incretin-based therapies are becoming the major player in the treatment of diabetes and obesity. Liraglutide and semaglutide are widely used around the world for weight reduction. The observed decrease in lipid overload affects not only subcutaneous fat but also internal organs (e.g. liver). Previous studies have found that lipid accumulation in cultured HepG2 cells (human hepatoma cells) can be alleviated by exenatide [12]. Incretin-based therapies were shown to effectively improve markers of steatohepatitis in diabetic, obese subjects [13]. Results of clinical trials also suggest that GLP-1 analogues might be implemented in the treatment of MASLD [1]. Furthermore, recent data indicate that an even greater impact on liver steatosis may be achieved by dual-receptor agonists. Cotadutide, which activates both the GLP-1 and glucagon receptors, exhibited promising results in animal models of liver steatosis. In a recently completed clinical trial in overweight diabetic subjects, cotadutide therapy was associated with a significant impact on liver steatosis and improvements in lipid and glucose metabolism [14]. Those effects seemed to be more pronounced than those of an active comparator — liraglutide.

Therefore, we conceived an *in vitro* study to assess the influence of dual receptor activation, using GLP-1 analogue (exenatide) and glucagon, on the free fatty acid-induced steatosis in human hepatoma cells. Our aim was to estimate the level of oxidative stress (ROS and MDA) induced by lipid overload and to evaluate the impact of exenatide and/or glucagon on the expression of antioxidant enzymes (SOD, GPx, Cat).

Material and methods

HepG2 culture conditions

HepG2 cells were obtained from a commercially available source (HB-8065, ATCC) from ATCC (Manassas, VA, USA) and cultivated (Heracell, Thermo Fisher Scientific, Inc., Grand Island, NY, USA) according to the manufacturer's recommendations [Dulbecco's Modified Eagle Medium (DMEM), Cat. No. 31966047, Gibco, Burlington, MA, USA] supplemented with 10% foetal bovine serum (Cat. No. 10500064, Gibco, MA, USA) and 1% penicillin/streptomycin (Cat. No. 15070063, Gibco, MA, USA) at 37ºC and 5% CO_2. The culture medium employed to induce steatosis contained 400 μM oleic acid (oleic acid BioReagent, Cat. No. 01383-10G Merck Sigma-Aldrich, Poznań, Poland) dissolved in 1% fatty acid free bovine serum albumin (BSA). Cells were seeded on 24-well plates (5×10^4) or 96-well plates (1×10^4) and cultured until reaching 70% confluence. Afterwards, on the day of the experiments, culture medium was replaced with a fresh one, supplemented with respective reagents: glucagon (Human glucagon EDQM, Cat. No. Y0000191-2EA Merck Sigma-Aldrich, Poznań, Poland) — 30 nM solution, exenatide (Exendin-4, Cat. No. E7144, Merck Sigma-Aldrich, Poznań, Poland) — 200 nM solution, or glucagon (30 nM) and exenatide (200 nM). The culture lasted for 24 h. All experiments were performed up to the 20th cell passage. The viability of cells exposed to all experimental conditions was estimated using 0.4% trypan blue method using a Bio-Rad TC-20 automated cell counter (Bio-Rad, Hercules, CA, USA). Briefly, 10 μL aliquots of trypsinised cell suspension was mixed with 10 μL of 0.4% trypan blue and incubated for 3 min. Afterwards, a 10-μL sample was injected into the sample plate and processed in the counter. Results were reported as a relative value to control sample.

Quantification of steatosis

An Oil Red O (ORO) technique was employed to assess the extent of lipid accumulation [Lipid (Oil Red O) Staining Kit, Cat. No. 194, Sigma-Aldrich St. Louis, USA]. After the experimental procedure, cells were immobilised on a culture plate by fixation with a 10% formalin solution for a duration of one hour. After rinsing with water and 60% isopropanol, an Oil Red O Working Solution was added, and cultures were incubated for 20 min, followed by 3 washes with water. Then cells were stained with haematoxylin for one min and washed 3 times with water. At this step the cells were evaluated using a Delta Optical IB-100 microscope (Delta Optical, Nowe Osiny, Poland) at 400× magnification. Finally, the stain was extracted from the wells with 100% isopropanol, and its amount was assessed at 492 nm wavelength on a spectroscope xMark Microplate Absorbance Spectrophotometer (Bio-Rad Laboratories, Hercules, CA., USA). Experiments were performed in duplicate.

Assessment of oxidative stress (ROS, MDA)

The ROS level was estimated using a commercially available kit (Fluorometric Intracellular ROS Kit, Cat. No. MAK143, Sigma-Aldrich, St. Louis, MO, USA). The assay detects predominantly superoxide and hydroxyl radicals. Cells were cultured on a 96-well plate in 90 μL of culture media. At the end of the experiment, each well was supplemented with 100 μL of Master Reaction Mix for 1 h. Afterwards, oxidative stress was induced by the addition of 10 μL of hydrogen peroxide (0.3%) and incubated for 30 min. The fluorescence intensity was measured on xMark Microplate Absorbance Spectrophotometer (BioRad Laboratories, Hercules, CA, USA) at 520 nm. The result is expressed as observed optical density (OD). Assays were run in duplicate.

Lipid peroxidation was assessed using a thiobarbituric acid (TBA) method with a commercially available kit [Lipid Peroxidation (MDA) Assay Kit, Cat. No. MAK085, Sigma-Aldrich, St. Louis, MO, USA]. Cells derived from 24-well plates were lysed with 300 μL of lysis buffer, transferred to vials and centrifuged at 13,000 g for 10 min. Then, 200 μL from each sample was transferred to a new vial, supplemented with 600 μL of TBA solution and incubated at 95ºC for 1 h. After cooling the samples to room temperature, 200-μL aliquots were transferred to a 96-well plate for analysis. The fluorescence intensity was measured on an xMark Microplate Absorbance Spectrophotometer (Bio-Rad Laboratories, Hercules, CA., USA) at 532 nm. The result is expressed as the observed optical density. Assays were done in duplicate.

Reverse transcription-quantitative polymerase chain reaction (RT-QPCR)

The assessment of SOD1, GPx and Cat were performed using quantitative polymerase chain reaction (QPCR). Primer sequences for SOD, GPx, and Cat were obtained from the PrimerBank database [15] *SOD1*: forward GAAGGTGTGGGGAAGCATTA; reverse CCACCGTGTTTTCTGGATAGA. *GPx*: forward-CGGGACTACACCCAGATGAA; reverse-TCTCTTCGTTCTTGGCGTTC. *Cat*: forward TCAGGCAGAAACTTTTCCATT; reverse TGGGTCGAAGGCTATCTGTT. Beta-actin (*ACTB*) gene was chosen as a reference gene for subsequent calculations. Primer sequences for RT-QPCR were sourced from the same repository as previously mentioned (PrimerBank), and they were as follows: *ACTB* forward: TCATGAAGTGTGACGTGGACATC, *ACTB* reverse: CAGGAGGAGCAATGATCTTGATCT. Total RNA was extracted from cultures of HepG2 cells by adding 1 mL of TRI reagent (MRC Inc., Cincinnati, OH, USA) to lyse cells derived from one of 24-well culture plates (5×10^4 cells per well) (SPL Life Sciences Co., Ltd., Immuniq, Żory, Poland) according to manufacturer's recommendations. The final amount of RNA was dissolved in 150 μL of nuclease-free water, and the concentration

and purity were measured spectrophotometrically at the wavelength of 260/280 nm (BioPhotometer, Eppendorf GmbH, Hamburg, Germany). To remove potential contamination with DNA, samples containing 2 μg of total RNA were exposed to DNase-I for 15 minutes at 37°C (RNase-free, Promega GmbH, Walldorf, Germany). Afterwards, 1 μg of DNA-free RNA was reverse transcribed and suspended in 20 μL of solution. In the final step of the procedure, it was further diluted by a factor of 5, as recommended by the manufacturer (GoScript Reverse Transcription System, Promega GmbH, Walldorf, Germany). RT-PCR reaction mixtures consisted of 10 μL of SYBR Select Master Mix (Thermo Fisher Scientific, Warsaw, Poland), 0.2 μM of each primer (SOD1 F/R or GPx F/R or Cat F/R), and 2 μL of reverse transcription mixture (equivalent of 10 ng of total RNA). A Roche LightCycler 480 Instrument II (Roche Diagnostics, Warsaw, Poland) with a specific thermal profile (94°C/3 min then 45 cycles of 94°C/30 s, 58°C/30 s, and 72°C/45 s) was used to estimate the level of gene expression. Specificity of products was confirmed using melting curve generation. Increasing fluorescence was measured in real-time to obtain the value of cycle threshold (CT), which was then normalised to that of ACTB expression and used for calculation of a relative gene expression, according to the $2^{(-\Delta\Delta Ct)}$ formula [16].

Western blot

Human-specific antibodies were used as follows: superoxide dismutase-1: Anti-SOD1 (Sigma, Cat. No. SAB1411305), glutathione peroxidase: Anti-GPX1 (Invitrogen, Cat. No. PA5-30593); catalase: Anti-Catalase (Thermo, Cat. No. PA5-29650); and β-actin (Sigma, Cat. No. SAB5600204). Cells were cultured on 24-well culture plates (5×10^4 cells per well) (SPL Life Sciences Co., Ltd.). Prior to cell lysis, plates were placed on ice, and cells were washed briefly with 500 μL of ice-cold PBS (phosphate-buffered saline). Protein extraction was done using 200 μL of cold RIPA (Radio-Immunoprecipitation Assay) buffer supplemented with 1.5 μL of Halt Protease Inhibition Cocktail (1:100 v/v) per well (both chemicals from Thermo Fischer Scientific, Inc., Warsaw, Poland). The total amount of protein was measured in each sample by bicinchoninic acid assay (BCA assay, Merck Millipore, Poznań, Poland), and the total protein concentration was calculated according to the standard curve based on BSA solutions of known protein concentration (Thermo Fisher Scientific, Inc., Warsaw, Poland). Proteins from cell lysates were separated by means of electrophoresis in polyacrylamide gel in the presence of ColorPlus Prestained Protein Marker (New England Biolabs, Lab-Jot, Warsaw, Poland), and 20 μg of total protein was loaded into gel slots. After separation, proteins were immediately electroblotted onto a PVDF membrane (Merck Millipore, Poznań, Poland). Membranes were blocked by incubation in 3% BSA solution in Tris-buffered saline (1X TBS) for 2 hours, and then membranes were placed in 3% BSA/1X TTBS (TBS supplemented with 0.05 % of Tween-20) containing one type of antibody at a final dilution of 1:1000. Incubations were performed for 1 h at ambient temperature with continuous rocking. Then, after 2 washes in TTBS for 10 min each, an Anti-rabbit IgG (whole molecule) peroxidase-conjugated, secondary antibody (No. Cat. A0545, Merck Millipore, Poznań, Poland) was added (antibody dilution: 1:10,000 in 3% BSA/TTBS). Incubation was performed for one hour under continuous rocking. Finally, after 3 washes (2X TTBS for 5 min each and 1X TBS for 5 min), a specific chemiluminescent signal was developed (Pierce ECL Western Blotting Substrate, Thermo Fisher Scientific, Inc., Warsaw, Poland). After development, membranes were digitised using the ChemiDoc-It Imaging System (Analytik Jena, Jena, Germany). Measurements of relative optical density (ROD) representing the amount of the protein of interest in a sample were done using ImageJ software [17].

Statistical analysis

The normality of distribution of data was evaluated using Shapiro-Wilk's test. All data were normally distributed and analysed using one-way t-test or ANOVA with post-hoc Tukey test and reported as means ± SEM. The p level below 0.05 was considered as statistically significant.

Results

Viability

The viability of HepG2 cells exposed to all experimental conditions remained unaffected (Fig. 1).

Induction of steatosis in cultured HepG2 cells

At the beginning of the study, we successfully induced cellular steatosis in HepG2 cells using oleic acid, which resulted in a major (64%) increase in intracellular lipid content (Fig. 2A).

In the following step, steatotic HepG2 cells were exposed to either glucagon, exenatide, or a combination of both. As a result, a statistically significant reduction (by 25%) in the lipid content was observed in cells treated with exenatide. However, the changes in cellular steatosis levels observed in cells exposed to glucagon alone or in combination with exenatide did not reach statistical significance compared to controls (Fig. 3A).

Markers of oxidative stress (ROS and MDA)

In the initial experiments we observed that exposure to oleic acid led to a significant (19%) increase in the level of ROS (Fig. 2B). Therefore, we estimated the influence of glucagon and exenatide in cultures exposed to oleic acid. None of the monotherapies affected the ROS level. The level of ROS was significantly reduced (by 24%) only in cells treated with both glucagon and exenatide (Fig. 4A). Importantly, we noted that combined therapy reduced the ROS level to a greater extent than gluca-

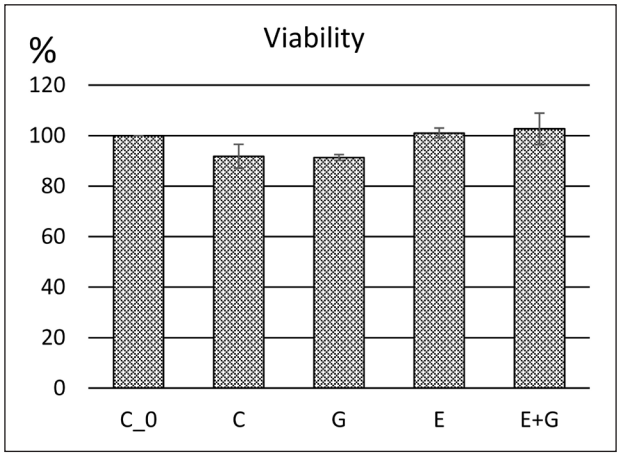

Figure 1. *Relative viability of HepG2 cells subjected to all experimental conditions: culture medium only (C_0); oleic acid (C); oleic acid and glucagon (G); oleic acid and exenatide (E); oleic acid, glucagon, and exenatide (E + G). Data are expressed as mean percentages ± standard error of the mean (SEM) in comparison to C_O (n = 3)*

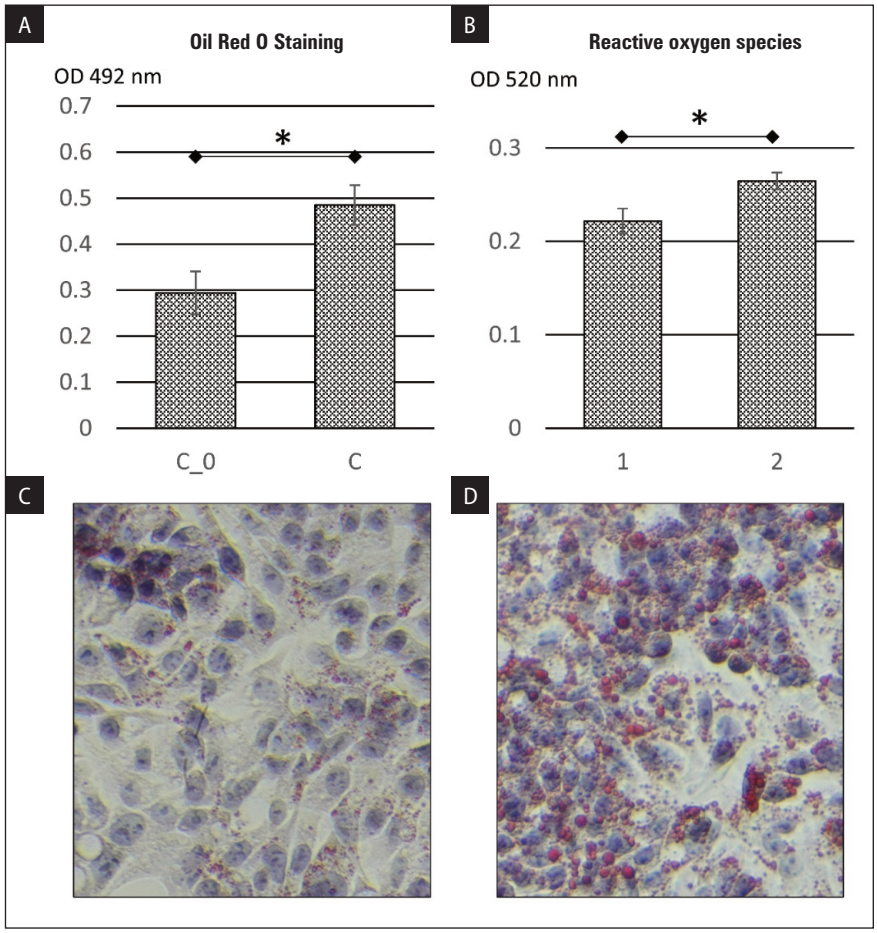

Figure 2. *Intracellular lipid accumulation in HepG2 cells. Figure shows representative microphotographs depicting lipid droplets stained by Oil Red O in control cultures (C_0) and cells exposed to oleic acid (C). Data are expressed as mean signal intensity ± standard error of the mean (SEM). The level of statistical significance is marked by an asterisk: *p < 0.05 (n = 6)*

gon or exenatide alone. The MDA level, which might be considered as a legacy of the ROS exposure, was effectively reduced by 21% in cells exposed to combined treatment with glucagon and exenatide (Fig. 4B). Contrary to observations in experiments on ROS levels, there was no additive impact of combined treatment versus monotherapies.

Antioxidant enzyme expression

SOD

Compared to controls, SOD mRNA expression was considerably increased in HepG2 cells exposed to exenatide monotherapy (nearly 4-fold) or both glucagon and exenatide treatment (5-fold). Glucagon alone was not able to change SOD mRNA expression (Fig. 5A). Interestingly, the impact on the expression of SOD protein seemed less pronounced. In contrast to controls, the difference reached statistical significance only in cultures exposed to both glucagon and exenatide (by 1.9-fold). Additionally, the combined treatment effectively increased SOD protein levels by 52% in HepG2 cells compared to treatment with glucagon alone (Fig. 5B).

GPx

The expression of GPx mRNA was substantially elevated in cultures exposed to both glucagon and exenatide, showing a 6.6-fold increase. Conversely, the impact of exenatide alone on GPx mRNA levels was less pronounced, with a 1.8-fold increase compared to controls (Fig. 5C). No measurable impact of glucagon alone on GPx mRNA expression was observed.

In experiments assessing GPx protein expression, a significant increase in GPx levels was observed only in HepG2 cell cultures exposed to both glucagon and exenatide, resulting in a 2-fold rise. However, neither of the monotherapies influenced GPx protein expression.

Cat

Interestingly, the experiments on expression of Cat showed that the mRNA level in cells subjected to glucagon and exenatide was modestly reduced by 32%. However, this finding was not translated into results

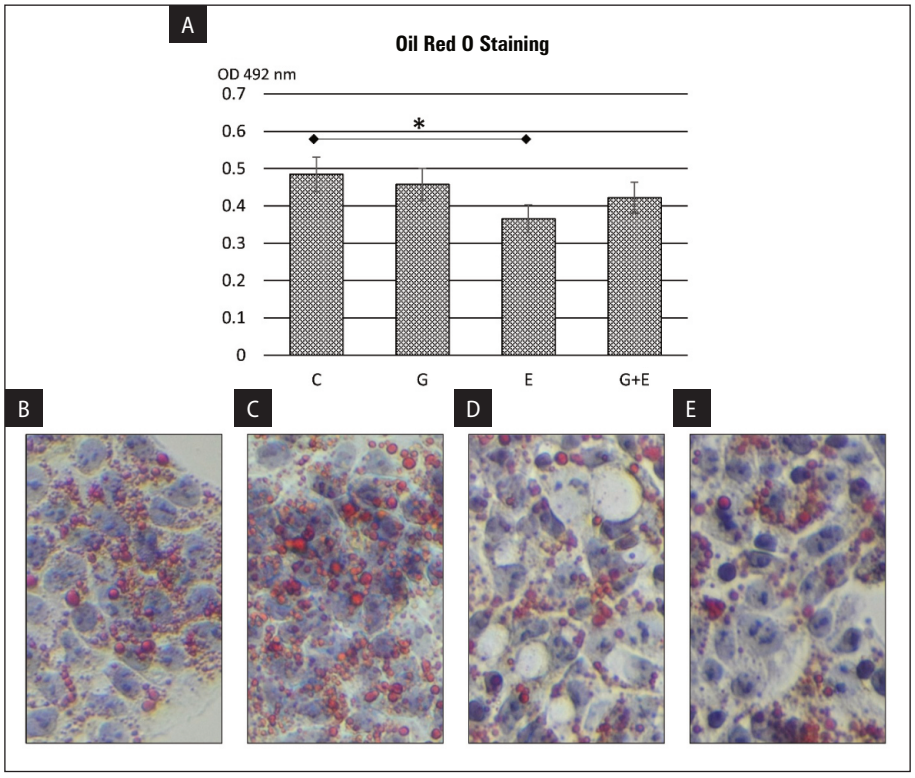

Figure 3. *The impact of glucagon (G), exenatide (E), and combined treatment (G + E) on the intracellular lipid accumulation in HepG2 cells exposed to oleic acid. Figure accompanied by representative microphotographs depicting lipid droplets stained by Oil Red O in selected culture conditions. Data are expressed as mean signal intensity ± standard error of the mean (SEM). The level of statistical significance is marked by an asterisk: *p < 0.05 (n = 6)*

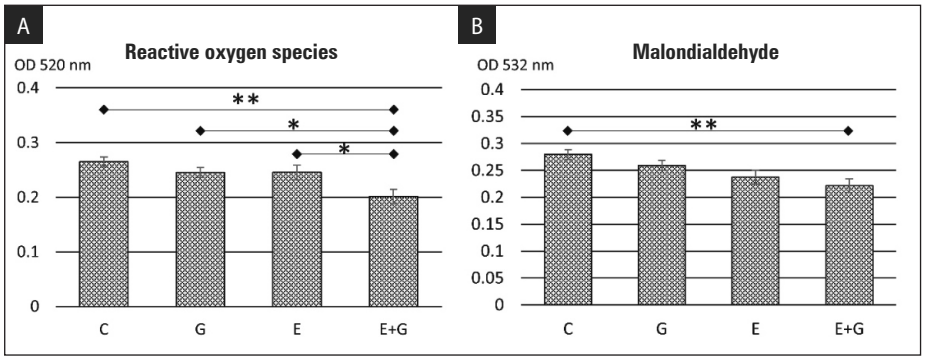

Figure 4. *The influence of glucagon (G), exenatide (E), and combined treatment (E + G) on the level of reactive oxygen species (ROS) (**A**) and malondialdehyde (MDA) (**B**). Data are expressed as mean signal intensity ± standard error of the mean (SEM). The level of statistical significance is marked by an asterisk: *p < 0.05, **p < 0.01, ***p < 0.001 (n = 6)*

of experiments involving the assessment of protein expression, which remained unaffected in all culture conditions.

Discussion

Our study showed that *in vitro* exposure of HepG2 cells to oleic acid resulted in intracellular lipid accumulation. To some extent, those changes resemble histological findings in the liver of patients with MASLD. The steatosis was associated with increased oxidative stress. The lipid burden was effectively reduced by exenatide treatment. However, to affect oxidative stress markers (ROS and MDA) both glucagon and exenatide had to be added to culture media. The reduction in oxidative stress was associated with an increased SOD and GPx, but not with Cat expression.

The progression of MASLD from simple steatosis to liver cirrhosis is a gradual process [1]. Up to 40% of patients with steatosis may progress into steato-

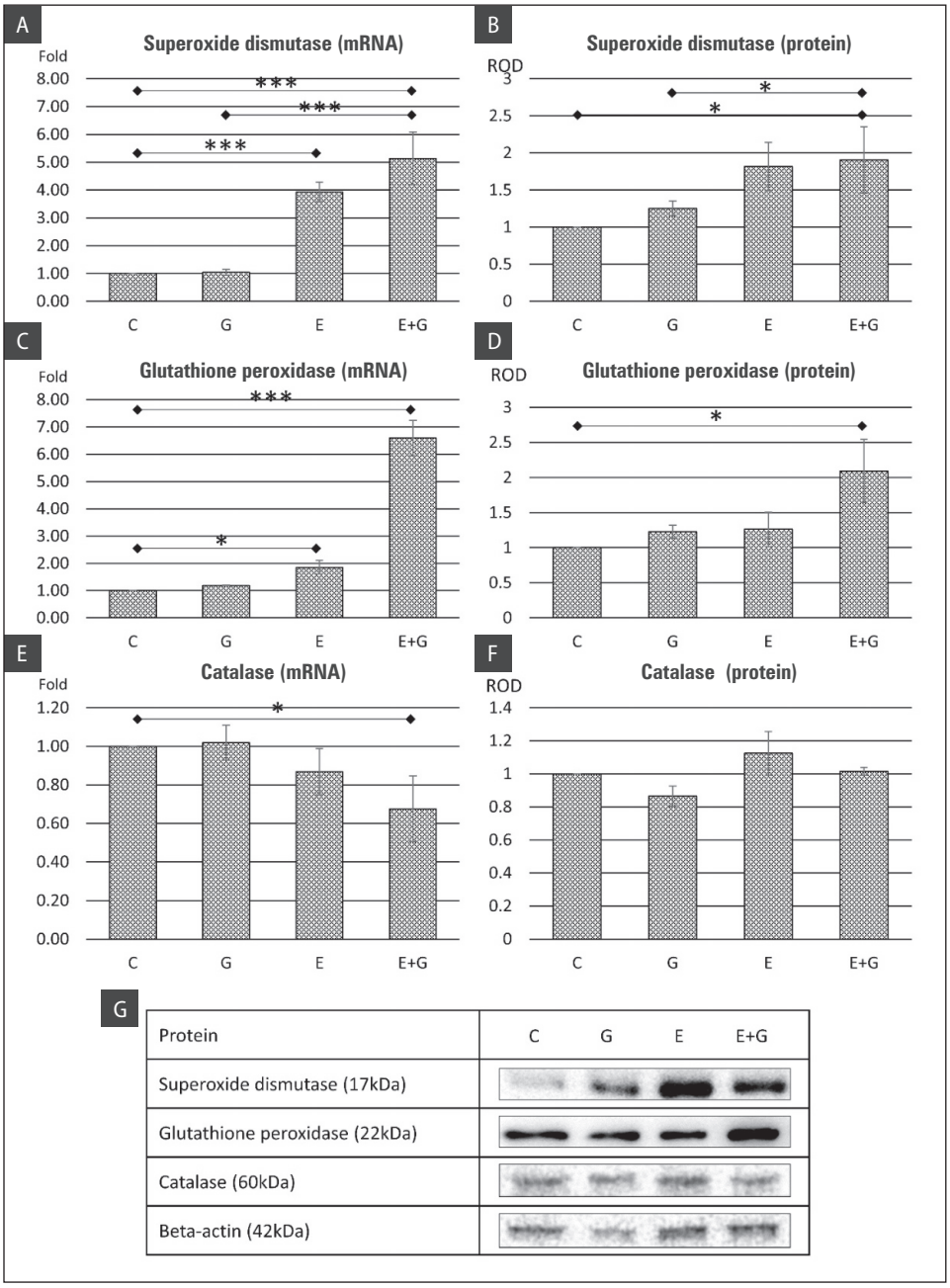

Figure 5. *The influence of glucagon (G), exenatide (E), and combined treatment (E + G) on the level of superoxide dismutase (SOD), glutathione peroxidase (GPx), and catalase (Cat) expression at the mRNA (***A***, ***C***, ***E***) and protein (***B***, ***D***, ***F***) level;* **G.** *Representative western blot bands. Data are expressed as mean relative values ± standard error of the mean (SEM). The level of statistical significance is marked by an asterisk: *p < 0.05, **p < 0.01, ***p < 0.001 (n = 5 for SOD and n = 4 for Cat and GPx)*

hepatitis. One of the potential links between those 2 conditions is oxidative stress leading to lipotoxicity arising from concurrent lipid accumulation. Previous *in vitro* studies showed excessive ROS generation accompanied by high triglyceride content in HepG2 cell cultures exposed to oleic and palmitic acids [18]. One of the sources for excessive oxidative stress is attributed to elevated expression of NADPH oxidase, which is a major source of intracellular ROS [19]. Lipid-laden hepatocytes were also shown to be affected by reduced antioxidant enzyme activities [20]. Other cells such as Kupfer cells also actively participate in oxidative status inside the liver [21]. Therefore, the cause of increased oxidative stress in the liver seems to be complex. In our experiments the increased level of ROS was associated with secondary lipid oxidation, which is expressed by MDA level — a well-established marker of lipid peroxidation [22]. In observational studies, elevated MDA level was associated with increased risk of progression of non-alcoholic fatty liver disease (NAFLD) toward

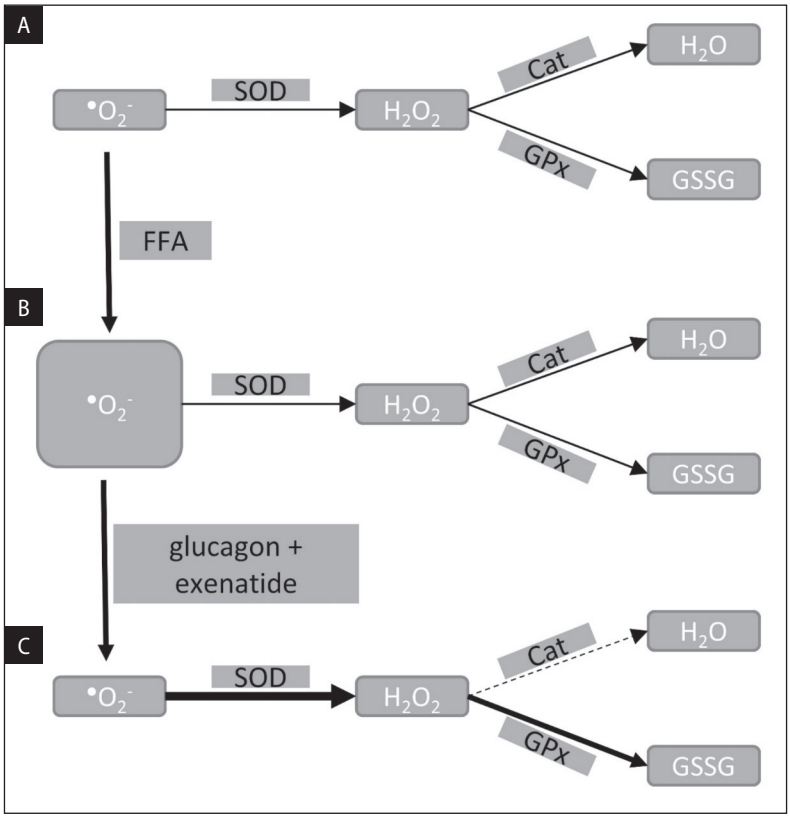

Figure 6. *Potential reactive oxygen species (ROS) scavenging pathways introduced during exposure of steatotic HepG2 cells to glucagon and exenatide. Control cells (***A***) subjected to free fatty acids (FFA) showed increased burden of oxidative stress (***B***), which was alleviated by addition of glucagon and exenatide to culture medium (***C***). O_2 — oxygen; SOD — superoxide dismutase; H_2O_2 — hydrogen peroxide; Cat — catalase; GPx — glutathione peroxidase; H_2O — water; GSSG — oxidised glutathione*

non-alcoholic steatohepatitis (NASH) and fibrosis [23]. Vitamin E (alpha-tocopherol), belonging to a group of potent antioxidants, is currently recommended in the treatment of MASH in patients without type 2 diabetes mellitus [24]. Therefore, it seems that moderation of lipid accumulation in hepatocytes and subsequent reduction in oxidative stress might be promising therapeutic options in MASLD. It is worth mentioning that vitamin E might exert some of its beneficial features in the course of MASLD by increasing the level of GLP-1 [25]. Benefits in the course of the experimental model of NAFLD in mice treated with other antidiabetic drugs like dapagliflozin (a sodium/glucose cotransporter 2 inhibitor) might also be attributed to incretin effects resulting from the inhibition of dipeptidyl peptidase-4 leading to subsequent GLP-1 availability [26].

Recently, a growing body of evidence suggests that improvements in the course of MASLD might be achieved by GLP-1 analogues [27]. These drugs were primarily indicated in the therapy of type 2 diabetes, but current indications include the treatment of obesity. During the therapy with GLP-1 analogue (dulaglutide), a 26.4% ($p = 0.004$) reduction in intrahepatic lipid content assessed by magnetic resonance [magnetic resonance imaging-derived proton density fat fraction (MRI-PDFF)] was noted. GLP-1 effects on steatosis were accompanied by a reduction in markers of oxidative stress (MDA) in an animal model [28]. However, it is not certain whether the beneficial impact on the liver relies on weight reduction or is related to the influence on oxidative stress. Previous studies on GLP-1 analogues showed its potent antioxidant and anti-inflammatory properties in monocytes/macrophages and pancreatic islet beta cells [29]. Among the explored *in vitro* mechanisms, the impact of protective effects of GLP-1 analogues on hepatocytes include activation of Nrf2 (nuclear factor E2-related factor 2) [30] and inhibition of NLRP3 (NOD-, LRP-, and pyrin domain-containing protein 3) inflammasome [31]. The former is associated with the expression of antioxidant enzymes. Real-world data showed that GLP-1 analogue can reduce the incidence of cirrhosis and hepatocellular carcinoma by 15% [0.85 (95% confidence interval (CI): 0.75–0.97)] [32]. In addition, novel dual-receptor agonists for GLP-1 and glucagon, such as cotadutide, have been shown to significantly improve hepatic inflammation [33] and liver function tests, with only a moderate impact on weight [34]. There is a scarcity of data exploring the impact of

GLP-1 and glucagon receptor agonists on the expression of antioxidant enzymes. In our experimental setting we found that elevated levels of SOD and GPx levels were achieved only in cells subjected to combined therapy with GLP-1 analogue and glucagon, whereas there was no change in catalase expression (Fig. 6).

This might be a result of the above-mentioned impact on the Nrf2 pathway [35] and the lipolytic properties of those drugs [36]. Therefore, based on our experiments, we believe that concurrent stimulation of GLP-1 and glucagon receptors enhances beneficial effects on cellular steatosis and oxidative stress in HepG2 to a greater extent than either monotherapy alone. These results show one of the mechanisms that might be responsible for *in vivo* improvements of liver steatosis and liver function tests.

The limitations of the study must be kept in mind. The *in vitro* nature of experiments, including only HepG2 cells, cannot reflect the complexity of cellular interactions inside the liver (e.g. stellate cells, Kupffer cells). Additionally, the choice of human neoplastic cellular line (HepG2) poses some risks in the extrapolation of data to an *in vivo* setting. However, several immortalised hepatic cell lines were used as an *in vitro* model for liver steatosis (HepG2, HepaRG, HuH7). The advantage of the HepG2 model is its relative simplicity of culture and proneness to lipid accumulation accompanied by significant expression of inflammatory cytokines and enzymes involved in redox status [37]. The shortcomings of HepG2 cells are their low activity and low inducibility of CYP450 cytochromes that are involved in the drug metabolism (but both exenatide and glucagon are not subject to CYP450 metabolism). In such studies it is recommend that HepaRG or primary human hepatocytes (PHHs) be used [38]. PHHs are considered a gold-standard in liver steatosis studies, but their usage has some limitations including invasive procedures required to obtain such cells (liver biopsy). One must also bear in mind that PHH cultures are composed of differentiated cells with limited life span, and due to different genetic or metabolic backgrounds the cultures tend to vary between specimens obtained from different individuals, which might render lower reproducibility between experiments [39]. Therefore, we believe that the setting used in our experiments depicts well the initial phase of MASLD — intracellular lipid accumulation, which at some point leads to activation of other cells involved in the progression of MASLD into advanced stages.

Conclusions

In our experiments a successful accumulation of lipids in HepG2 cells was achieved. Increased intracellular content was associated with increased oxidative stress. Exenatide reduced the extent of intracellular lipid accumulation, while combined treatment with glucagon and exenatide was able to alleviate oxidative stress. We speculate that this observation was a result of increased antioxidant enzyme expression (SOD and GPx).

Data availability statement

All data are included in the manuscript

Ethics statement

The study required no ethics board approval — *in vitro* study.

Author contributions

A.B. — conceived the study, analysed data, wrote manuscript; LB — performed experiments, wrote manuscript, reviewed manuscript; ES — performed cultures and contributed to experiments; GM — performed experiments, contributed to discussion; BO — overviewed experiments, contributed to discussion.

Funding

Statutory grant from Medical University of Silesia (Grant No. BNW-1-031/N/3/O).

Conflict of interest

The authors declare no conflict of interests.

References

1. Bołdys A, Bułdak Ł, Maligłówka M, et al. Potential Therapeutic Strategies in the Treatment of Metabolic-Associated Fatty Liver Disease. Medicina (Kaunas). 2023; 59(10), doi: 10.3390/medicina59101789, indexed in Pubmed: 37893507.
2. Avcı E, Kucukoduk A. Choroidal vascular changes in non-alcoholic fatty liver disease. Endokrynol Pol. 2023; 74(4): 430–436, doi: 10.5603/ep.95686, indexed in Pubmed: 37823522.
3. Belli LS, Perricone G, Adam R, et al. all the contributing centers (www.eltr.org) and the European Liver and Intestine Transplant Association (ELITA). Impact of DAAs on liver transplantation: Major effects on the evolution of indications and results. An ELITA study based on the ELTR registry. J Hepatol. 2018; 69(4): 810–817, doi: 10.1016/j.jhep.2018.06.010, indexed in Pubmed: 29940268.
4. Wong RJ, Aguilar M, Cheung R, et al. Nonalcoholic steatohepatitis is the second leading etiology of liver disease among adults awaiting liver transplantation in the United States. Gastroenterology. 2015; 148(3): 547–555, doi: 10.1053/j.gastro.2014.11.039, indexed in Pubmed: 25461851.
5. van Herpen NA, Schrauwen-Hinderling VB. Lipid accumulation in non-adipose tissue and lipotoxicity. Physiol Behav. 2008; 94(2): 231–241, doi: 10.1016/j.physbeh.2007.11.049, indexed in Pubmed: 18222498.
6. Mello T, Zanieri F, Ceni E, et al. Oxidative Stress in the Healthy and Wounded Hepatocyte: A Cellular Organelles Perspective. Oxid Med Cell Longev. 2016; 2016: 8327410, doi: 10.1155/2016/8327410, indexed in Pubmed: 26788252.
7. Delli Bovi AP, Marciano F, Mandato C, et al. Oxidative Stress in Non-alcoholic Fatty Liver Disease. An Updated Mini Review. Front Med (Lausanne). 2021; 8: 595371, doi: 10.3389/fmed.2021.595371, indexed in Pubmed: 33718398.
8. Pandey KB, Rizvi SI. Markers of oxidative stress in erythrocytes and plasma during aging in humans. Oxid Med Cell Longev. 2010; 3(1): 2–12, doi: 10.4161/oxim.3.1.10476, indexed in Pubmed: 20716923.
9. Bułdak Ł, Łabuzek K, Bułdak RJ, et al. Exenatide (a GLP-1 agonist) improves the antioxidative potential of in vitro cultured human monocytes/macrophages. Naunyn Schmiedebergs Arch Pharmacol. 2015; 388(9): 905–919, doi: 10.1007/s00210-015-1124-3, indexed in Pubmed: 25980358.
10. Bułdak Ł, Machnik G, Skudrzyk E, et al. The impact of exenatide (a GLP-1 agonist) on markers of inflammation and oxidative stress in normal human astrocytes subjected to various glycemic conditions. Exp Ther Med. 2019; 17(4): 2861–2869, doi: 10.3892/etm.2019.7245, indexed in Pubmed: 30906473.

11. Bułdak Ł, Skudrzyk E, Machnik G, et al. Exenatide improves antioxidant capacity and reduces the expression of LDL receptors and PCSK9 in human insulin secreting 1.1E7 cell line subjected to hyperglycemia and oxidative stress. Postepy Hig Med Dosw . 2022; 76(1): 16–23, doi: 10.2478/ahem2021-0037.
12. Khalifa O, H Mroue K, Mall R, et al. Investigation of the Effect of Exendin-4 on Oleic Acid-Induced Steatosis in HepG2 Cells Using Fourier Transform Infrared Spectroscopy. Biomedicines. 2022; 10(10), doi: 10.3390/biomedicines10102652, indexed in Pubmed: 36289914.
13. Nahra R, Wang T, Gadde KM, et al. Effects of Cotadutide on Metabolic and Hepatic Parameters in Adults With Overweight or Obesity and Type 2 Diabetes: A 54-Week Randomized Phase 2b Study. Diabetes Care. 2021; 44(6): 1433–1442, doi: 10.2337/dc20-2151, indexed in Pubmed: 34016612.
14. Parker VER, Robertson D, Erazo-Tapia E, et al. Cotadutide promotes glycogenolysis in people with overweight or obesity diagnosed with type 2 diabetes. Nat Metab. 2023; 5(12): 2086–2093, doi: 10.1038/s42255-023-00938-0, indexed in Pubmed: 38066113.
15. Spandidos A, Wang X, Wang H, et al. PrimerBank: a resource of human and mouse PCR primer pairs for gene expression detection and quantification. Nucleic Acids Res. 2010; 38(Database issue): D792–D799, doi: 10.1093/nar/gkp1005, indexed in Pubmed: 19906719.
16. Livak KJ, Schmittgen TD. Analysis of relative gene expression data using real-time quantitative PCR and the 2(-Delta Delta C(T)) Method. Methods. 2001; 25(4): 402–408, doi: 10.1006/meth.2001.1262, indexed in Pubmed: 11846609.
17. Schindelin J, Arganda-Carreras I, Frise E, et al. Fiji: an open-source platform for biological-image analysis. Nat Methods. 2012; 9(7): 676–682, doi: 10.1038/nmeth.2019, indexed in Pubmed: 22743772.
18. Maseko TE, Elkalaf M, Peterová E, et al. Comparison of HepaRG and HepG2 cell lines to model mitochondrial respiratory adaptations in nonalcoholic fatty liver disease. Int J Mol Med. 2024; 53(2), doi: 10.3892/ijmm.2023.5342, indexed in Pubmed: 38186319.
19. Chen X, Li L, Liu X, et al. Oleic acid protects saturated fatty acid mediated lipotoxicity in hepatocytes and rat of non-alcoholic steatohepatitis. Life Sci. 2018; 203: 291–304, doi: 10.1016/j.lfs.2018.04.022, indexed in Pubmed: 29709653.
20. Li T, Gong H, Zhan B, et al. Chitosan oligosaccharide attenuates hepatic steatosis in HepG2 cells via the activation of AMP-activated protein kinase. J Food Biochem. 2022; 46(5): e14045, doi: 10.1111/jfbc.14045, indexed in Pubmed: 35187676.
21. Myint M, Oppedisano F, De Giorgi V, et al. Inflammatory signaling in NASH driven by hepatocyte mitochondrial dysfunctions. J Transl Med. 2023; 21(1): 757, doi: 10.1186/s12967-023-04627-0, indexed in Pubmed: 37884933.
22. Tsikas D. Assessment of lipid peroxidation by measuring malondialdehyde (MDA) and relatives in biological samples: Analytical and biological challenges. Anal Biochem. 2017; 524: 13–30, doi: 10.1016/j.ab.2016.10.021, indexed in Pubmed: 27789233.
23. Zelber-Sagi S, Ivancovsky-Wajcman D, Fliss-Isakov N, et al. Serum Malondialdehyde is Associated with Non-Alcoholic Fatty Liver and Related Liver Damage Differentially in Men and Women. Antioxidants (Basel). 2020; 9(7), doi: 10.3390/antiox9070578, indexed in Pubmed: 32630732.
24. Rinella ME, Neuschwander-Tetri BA, Siddiqui MS, et al. AASLD Practice Guidance on the clinical assessment and management of nonalcoholic fatty liver disease. Hepatology. 2023; 77(5): 1797–1835, doi: 10.1097/HEP.0000000000000323, indexed in Pubmed: 36727674.
25. Sun T, Zhang B, Ru QJ, et al. Tocopheryl quinone improves non-alcoholic steatohepatitis (NASH) associated dysmetabolism of glucose and lipids by upregulating the expression of glucagon-like peptide 1 (GLP-1) restoring the balance of intestinal flora in rats. Pharm Biol. 2021; 59(1): 723–731, doi: 10.1080/13880209.2021.1916542, indexed in Pubmed: 34139927.
26. Zhao Z, Zhao F, Zhang Y, et al. Risk factors of dapagliflozin-associated diabetic ketosis/ketoacidosis in patients with type 2 diabetes mellitus: A matched case-control study. Diabetes Res Clin Pract. 2023; 196: 110236, doi: 10.1016/j.diabres.2023.110236, indexed in Pubmed: 36610546.
27. Gu Y, Sun L, He Y, et al. Comparative efficacy of glucagon-like peptide 1 (GLP-1) receptor agonists, pioglitazone and vitamin E for liver histology among patients with nonalcoholic fatty liver disease: systematic review and pilot network meta-analysis of randomized controlled trials. Expert Rev Gastroenterol Hepatol. 2023; 17(3): 273–282, doi: 10.1080/17474124.2023.2172397, indexed in Pubmed: 36689199.
28. Gao H, Zeng Z, Zhang H, et al. The Glucagon-Like Peptide-1 Analogue Liraglutide Inhibits Oxidative Stress and Inflammatory Response in the Liver of Rats with Diet-Induced Non-alcoholic Fatty Liver Disease. Biol Pharm Bull. 2015; 38(5): 694–702, doi: 10.1248/bpb.b14-00505, indexed in Pubmed: 25947915.
29. Buldak L, Machnik G, Skudrzyk E, et al. Exenatide prevents statin-related LDL receptor increase and improves insulin secretion in pancreatic beta cells (1.1E7) in a protein kinase A-dependent manner. J Appl Biomed. 2022; 20(4): 130–140, doi: 10.32725/jab.2022.015, indexed in Pubmed: 36708718.
30. Zhu CG, Luo Y, Wang H, et al. Liraglutide Ameliorates Lipotoxicity-Induced Oxidative Stress by Activating the NRF2 Pathway in HepG2 Cells. Horm Metab Res. 2020; 52(7): 532–539, doi: 10.1055/a-1157-0166, indexed in Pubmed: 32375182.
31. Yu X, Hao M, Liu Yu, et al. Liraglutide ameliorates non-alcoholic steatohepatitis by inhibiting NLRP3 inflammasome and pyroptosis activation via mitophagy. Eur J Pharmacol. 2019; 864: 172715, doi: 10.1016/j.ejphar.2019.172715, indexed in Pubmed: 31593687.
32. Engström A, Wintzell V, Melbye M, et al. Association of glucagon-like peptide-1 receptor agonists with serious liver events among patients with type 2 diabetes: A Scandinavian cohort study. Hepatology. 2024; 79(6): 1401–1411, doi: 10.1097/HEP.0000000000000712, indexed in Pubmed: 38085855.
33. Patel V, Joharapurkar A, Kshirsagar S, et al. Coagonist of GLP-1 and glucagon decreases liver inflammation and atherosclerosis in dyslipidemic condition. Chem Biol Interact. 2018; 282: 13–21, doi: 10.1016/j.cbi.2018.01.004, indexed in Pubmed: 29325849.
34. Nahra R, Wang T, Gadde KM, et al. Effects of Cotadutide on Metabolic and Hepatic Parameters in Adults With Overweight or Obesity and Type 2 Diabetes: A 54-Week Randomized Phase 2b Study. Diabetes Care. 2021; 44(6): 1433–1442, doi: 10.2337/dc20-2151, indexed in Pubmed: 34016612.
35. Xue Y, Wei Y, Cao L, et al. Protective effects of scutellaria-coptis herb couple against non-alcoholic steatohepatitis via activating NRF2 and FXR pathways in vivo and in vitro. J Ethnopharmacol. 2024; 318(Pt A): 116933, doi: 10.1016/j.jep.2023.116933, indexed in Pubmed: 37482263.
36. Kiani B, Yarahmadi S, Nabi-Afjadi M, et al. Comprehensive Review on the Metabolic Cooperation Role of Nuclear Factor E2-Related Factor 2 and Fibroblast Growth Factor 21 against Homeostasis Changes in Diabetes. Clin Diabetol. 2022; 11(6): 409–419, doi: 10.5603/DK.a2022.0051.
37. Müller F, Sturla S. Human in vitro models of nonalcoholic fatty liver disease. Curr Opin Toxicol. 2019; 16: 9–16, doi: 10.1016/j.cotox.2019.03.001.
38. Gerets HHJ, Tilmant K, Gerin B, et al. Characterization of primary human hepatocytes, HepG2 cells, and HepaRG cells at the mRNA level and CYP activity in response to inducers and their predictivity for the detection of human hepatotoxins. Cell Biol Toxicol. 2012; 28(2): 69–87, doi: 10.1007/s10565-011-9208-4, indexed in Pubmed: 22258563.
39. Huggett ZJ, Smith A, De Vivo N, et al. A Comparison of Primary Human Hepatocytes and Hepatoma Cell Lines to Model the Effects of Fatty Acids, Fructose and Glucose on Liver Cell Lipid Accumulation. Nutrients. 2022; 15(1), doi: 10.3390/nu15010040, indexed in Pubmed: 36615698.